

Research Article

Seismic Performance of Super High-Rise Building Structure with Dual Lines of Defense Based on Response Surface Optimization Algorithm

Lei Zheng , Zonghui Liu , Hongwei Dang , Xin Guo , and Yonghua Wu 

Installation Engineering Co. Ltd. of CSCEC 7th Division, Zhengzhou 450000, China

Correspondence should be addressed to Lei Zheng; zhenglei@mjc-edu.cn

Received 11 July 2022; Revised 26 August 2022; Accepted 5 September 2022; Published 15 September 2022

Academic Editor: S. Mahdi S. Kolbadi

Copyright © 2022 Lei Zheng et al. This is an open access article distributed under the Creative Commons Attribution License, which permits unrestricted use, distribution, and reproduction in any medium, provided the original work is properly cited.

In order to improve the safety performance of supertall buildings under earthquake, a seismic performance analysis method of double lines of supertall buildings based on a response surface optimization algorithm is proposed. Firstly, the structural performance indexes of super high-rise buildings are selected, and on this basis, the material constitutive model is constructed by the structural elastic-plastic analysis method to complete the seismic design of the first line of defense. Then, the response surface method is used to optimize the material constitutive model and complete the seismic design of the second line. Finally, the anticollapse limit state analysis method is used to determine the seismic performance of the double line of super high-rise building structures. The experimental results show that the proposed analysis method has high seismic performance, and the axial compression ratio of wall and column is always stable, in which the column is always at about 0.5 and the wall is always at about 0.26, which lays a foundation for the safety performance of super high-rise building structures under earthquake.

1. Introduction

Earthquakes are one of the most serious natural disasters faced by mankind. According to incomplete statistics, in the past 100 years, dozens of cities around the world were destroyed by earthquake disasters, causing great casualties and property losses. Since ancient times, China has been a country with many earthquakes, with high frequency, intensity, and wide range of seismic activities. At 14:28 on May 12, 2008, a magnitude 8.0 earthquake occurred in Wenchuan County, Sichuan Province, my country, causing huge casualties and property losses. It was the most extensive and largest loss earthquake since the founding of the People's Republic of China. As an expert from the University of Colorado in the United States said, "it is building that causes casualties, not earthquakes." The destruction and collapse of a large number of super high-rise buildings are the main reasons for the huge casualties and property losses in this earthquake. Therefore, improving the seismic resistance of super high-rise building structures is a key factor in

enhancing the earthquake resistance and disaster prevention capabilities of earthquake areas and reducing earthquake losses. The types of super high-rise buildings mainly include large chassis, large podiums, and point buildings. Their structural systems include tube structure (including beam tube, tube in tube, frame-tube structure), steel-concrete mixed structure, shear wall structure, frame-supported shear wall structure, and frame-shear wall structure [1–3]. For high-intensity areas, shear wall structures are often used for residential structures between 100 and 150 m. In order to meet the seismic requirements of super high-rise buildings with dual lines of defense, the bearing capacity, rigidity, stability, energy absorption, and dissipation of the reinforced concrete building structure should meet the requirements under the action of earthquakes [4, 5]. In the seismic design of reinforced concrete houses, in addition to rational structure selection and correct structural measures, more attention should be paid to conceptual design. The goal of the dual-line-of-defense seismic design of super high-rise buildings is to make the overall structure play a role in

dissipating seismic energy, avoiding sensitive weak parts of the structure, leading to premature failure of super high-rise buildings [6–8].

In accordance with the original Ministry of Construction Order No. 111 of 2002, “Regulations on the Antiseismic Fortification Management of Over-limit High-rise Buildings” and the Ministry of Housing and Urban-Rural Development Construction Quality (2010) No. 109 Document “Special Technical Points for Seismic Fortification of Over-limit High-rise Buildings”, the notice requires that designers need to perform detailed calculations and demonstrations based on the actual over-limit conditions of specific over-limit high-rise buildings. Model tests are also required if necessary. The design personnel’s demonstrations also need to undergo a special review of seismic fortification to ensure the super high-rise building structure [9] and antiseismic safety performance with dual lines of defense. Li [10] analyzed the seismic performance of over-limit high-rise structures under moderate earthquakes. Taking a super high-rise steel-concrete column-reinforced concrete core tube hybrid structure as the engineering background, the three-dimensional space model was established by SATWE software, and the frame beam, connecting beam, and the shear wall are subjected to moderate earthquake nonyielding analysis, and the bottom through-height wall and column shear performance are subjected to moderate earthquake elastic analysis. The results show that the vertical members basically maintain good elastic properties, and a few members of the frame beams and coupling beams show bending yield. But not serious, and the shear resistance is still in the elastic stage, which can meet the requirements of nonyielding under moderate earthquakes. At the same time, under the action of moderate earthquakes, the coupling beams yield before the frame beams, and then the shear wall plastic hinge area yields. During the process, the frame column did not yield, which was consistent with the basic requirements of the second line of defense for seismic fortification. Yi and Zhou [11] analyzed the seismic performance of frame-shear wall structures with different frame overturning moment ratios and designed 8 frame-shear wall structure models with different frame overturning moment ratios according to the structural design specifications. Based on the fiber model, the PERFORM 3D program was used. The elastoplastic time history analysis of the example model under major earthquakes is carried out to study the influence of the frame overturning moment ratio on the overall seismic performance of the structure from various aspects. The results show that the frame-shear frame with the frame overturning moment ratio is between 15% and 60%. There is no significant difference in the seismic performance of the force wall structure, and when the frame overturning moment ratio is greater than 80%, the shear wall cannot be the first seismic line of defense of the frame-shear wall structure. However, the results of the above-mentioned two methods for the analysis of the antiseismic performance of the double line of defense of the super high-rise building structure are not good. Reference [12] proposes a damage tolerance solution to improve the seismic performance of buildings. To achieve this with minimal initial investment, the structure is

designed using the principle of ductility to experience significant plastic deformation in the primary structural elements. If structural damage is to some extent clearly accepted and quantifiable in design codes, then issues related to nonstructural damage will be dealt with more vaguely, which is no longer in line with market and society requirements. There is a need for new structural systems that not only effectively reduce structural and nonstructural damage but also provide good recentering capability, durability, reparability, and affordability while allowing for easy-to-use design approaches. Suwondo et al. [13] present a nonlinear analysis of the seismic performance of low-rise concrete buildings in Indonesia. This study uses nonlinear analysis to evaluate low-rise reinforced concrete buildings, and its main purpose is to investigate the actual safety level of concrete buildings that are seismically designed according to Indonesian standards. The results show that the building meets the expected goals of seismic design in both global and local responses.

On the basis of the above two methods, this paper proposes a method for analyzing the antiseismic performance of super high-rise buildings with dual lines of defense based on a response surface optimization algorithm; the innovation of this method is to select the structural performance index of super high-rise buildings and, at the same time, to build the material constitutive model by using the structural elastoplastic analysis method to complete the antiseismic design of the first line of defense. Then, the response surface method is used to optimize the material constitutive model and complete the seismic design of the second line of defense. Finally, the anticollapse limit state analysis method is used to determine the seismic performance of the double line of defense of the super high-rise building structure. The effectiveness of this method is verified by simulation experiments, which lays a foundation for the seismic safety performance of super high-rise buildings [14, 15].

2. Seismic Performance of Super High-Rise Building Structure with Dual Lines of Defense Based on Response Surface Optimization Algorithm

Response surface optimization algorithm is a statistical algorithm that uses reasonable experimental design methods and obtains certain data through experiments, uses multiple quadratic regression equation to fit the functional relationship between factors and response values, and seeks the optimal process parameters through the analysis of regression equation to solve multivariable problems. Response surface optimization (RSO) is a method for optimizing experimental conditions, which is suitable for solving the related problems of nonlinear data processing. It includes many test and design technologies such as test design, modeling, checking the suitability of the model, and seeking the best combination conditions. Through the regression fitting of the process and the drawing of the response surface and contour line, the response value corresponding to each

factor level can be easily obtained. Based on the response value of each factor level, the predicted optimal response value and corresponding experimental conditions can be found. The advantage of the response surface optimization algorithm is that the random error of the test is considered. At the same time, the complex unknown function relationship is fitted with a simple one- or two-degree polynomial model in a small area, which is easy to calculate and is an effective means to solve practical problems [16, 17].

The key to analyzing the seismic performance of super high-rise buildings lies in two points: one is the selection of reasonable structural performance indicators, and the failure degree of components is determined by performance indicators; the other is structural elastoplastic analysis, which calculates the deformation and internal force of the structure under a large earthquake distributed. Based on the selection of structural performance indicators, this paper uses structural elastoplastic analysis to construct a material constitutive model, completes the seismic design of the first line of defense, then uses the response surface method to optimize the material constitutive model, and completes the second line of defense. The anticollapse limit state analysis method is used to judge the seismic performance of super high-rise buildings with dual lines of defense. An antiseismic structural system should be composed of thousands of subsystems with good ductility and be connected by structural members with good ductility to work together. For example, the frame antiseismic wall system is composed of two systems: the ductile frame and the antiseismic wall. The double limb or multilimb seismic wall system is composed of ten single limb wall subsystems. The seismic structure system shall have the maximum possible internal and external redundancy and consciously establish a series of distributed yield zones so that the structure can absorb and dissipate a large amount of seismic energy, and it is easy to repair once damaged. If the building adopts multiple lines of defense, after the antilateral force members of the first line of defense are damaged under the strong earthquake attack, the antilateral force members of the second line of defense will be replaced immediately to withstand the impact of the subsequent ground motion, which can ensure the minimum safety of the building and avoid collapse [18, 19].

2.1. Deformation Index Limits of Super High-Rise Building Structural Members. This paper analyzes the antiseismic performance of the dual line of defense of the super high-rise building structure under the action of the earthquake by means of component deformation [20]. The structural components of super high-rise buildings include shear wall and beam components and determine the plane layout of the structure, including the structural column spacing, core tube size, coupling beam layout, frame column, beam number, and other pieces of information. Then, the structural member size is preliminarily estimated according to the structural floor load, and the design conditions of the structure are checked in the next step, such as the axial compression ratio of the vertical members of the structure, the displacement angle between the layers of the structure,

the period ratio, the stiffness weight ratio, the lateral stiffness ratio, the shear weight ratio of the floors, and the shear bearing capacity ratio. If the specification limits are not met, the corresponding components need to be modified and recalculated and recheck whether the limits of each design condition are met. When all design conditions meet the specification requirements, the size of the component can be determined. Finally, the reinforcement is carried out according to the internal force calculation results of the members. If the reinforcement ratio does not meet the requirements of the specification, it is necessary to change the section size of the member or improve the reinforcement strength. After recalculation, each condition shall be checked again until the conditions are met [21].

2.1.1. Shear Wall Deformation Performance Index Limit.

Because the shear failure is a brittle failure, the ductility is small, the boundary of each performance state is blurred, and the measured data about the shear performance of reinforced concrete is less, so only the wall members in the shear force state are not severely damaged. Deformation limits no longer give details of the deformation limits of other performance levels [22]. At the same time, in order to ensure the safety of the wall members under shear stress, the bearing capacity control principle is also adopted, and the performance of the wall members under shear stress is jointly controlled by the shear bearing capacity check calculation and the minimum shear section requirements.

The expression of shear wall shear capacity is

$$V \leq \frac{1}{\lambda - 0.5} \left(0.4 f_t b_w h_{w0} - 0.1 N \frac{A_{sh}}{S} \right) + 0.8 f_{yh} \frac{A_{sh}}{S} h_{w0}. \quad (1)$$

In the equation, N represents the standard value of the axial force of the shear wall, which is positive in tension and negative in compression. When N is pressure and the absolute value is greater than $0.2 f_c b_w h_w$, take $0.2 f_c b_w h_w$. When N is tension and the calculated value at the right end of (1) is less than $0.8 f_{yh} A_{sh} / S h_{w0}$, take $0.8 f_{yh} A_{sh} / S h_{w0}$. A represents the full cross-sectional area of shear wall members; A_{sh} represents the area of T -shaped or I -shaped cross section shear wall webs; λ represents the shear span ratio; S represents the spacing of horizontally distributed steel bars in the shear wall.

The expression of the minimum shear section is

$$V \leq 0.15 f_c b h_0. \quad (2)$$

In the equation, f_c represents the standard value of concrete axial compressive strength; b represents the width of the component section; h_0 represents the effective height of the component section [2]. The limit value of the deformation performance index of the shear wall can be obtained through the above equation. In order to ensure the safety of wall limb members in a shear stress state, the performance of wall limb members in a shear stress state is controlled jointly by shear bearing capacity checking calculation and minimum shear section requirements [23].

2.1.2. Deformation Performance Index Limit of Beam Member. For beam members under shear stress, the deformation limit is the same as that of shear walls; that is, only the deformation limit that is not severely damaged is specified. At the same time, the bearing capacity control principle is adopted, and the shear bearing capacity check calculation and the minimum shear section requirement are shared controlling the performance of beam members under shear stress.

Shear capacity of beam members is

$$V \leq 0.7 f_t b h_0 + f_{yv} \frac{A_{sv}}{S} h_0. \quad (3)$$

In the equation, f_t represents the axial tensile strength of concrete; b represents the width of the component section; h_0 represents the effective height of the component section; f_{yv} represents the tensile strength of the stirrups; S represents the stirrup spacing along the length of the component [24].

2.1.3. Classification Standard of Component Performance Status. Through the “Building Seismic Damage Grade Classification Standard”, the performance level of super high-rise building structural components is divided into five damage states: intact, slight damage, light and medium damage, medium damage, and nonserious damage [25–27]. In order to facilitate the analysis of the seismic performance of the super high-rise building structure, this paper divides the structural performance into two criteria according to the failure type. One is bending or bending and shear failure, and the components are classified by the deformation index. The other is a shear failure which is adopted. The minimum shear section requires that the control member does not undergo brittle failure. When the component is damaged by bending or bending and shear, the damage of the component is divided into six properties, namely, performance 1 to performance 6. When the component exceeds the nonserious damage limit, the component is defined as a serious damage. The specific meaning is shown in Figure 1. When the damage of the component exceeds Performance 5, it indicates that the bearing capacity of the component has entered the descending section, and the bearing capacity has dropped by more than 20%.

When a member undergoes shear failure, the member is divided into two states, namely, nonshear failure and shear failure, by the restriction condition of the minimum shear section. Due to the plastic deformation of the component, the bearing capacity limit equation is no longer suitable for describing the ultimate bearing capacity of the component. When the component does not meet the minimum shear section requirements, it indicates that the component has undergone brittle shear failure [28, 29].

2.2. Determination of Seismic Performance Based on the Analysis Method of Structural Collapse Resistance Limit State. The collapse resistance limit state analysis method is an incremental dynamic analysis method (Incremental Dynamic Analysis, IDA method for short), which was proposed by Bertero in 1977. The IDA method refers to the input of the

seismic time history of gradually increasing intensity, the elastoplastic analysis of the whole process from the structure to the collapse, and the determination of the collapse resistance limit state of the model. This section introduces the structural safety reserve coefficient R against collapse as a parameter to measure the structural safety reserve, which can determine the seismic performance of the double line of defense of the super high-rise building structure. Its expression is

$$R = \frac{IM_c}{IM_{MCE}}. \quad (4)$$

In the equation, IM_c represents the ground motion intensity at which the structure just reaches the collapse resistance limit state. IM_{MCE} represents the intensity of ground motion of the structure under rare earthquakes, determining the collapsed state of the structure according to the safety judgment principle of the super high-rise building.

When $R > 1$, it indicates that the structure has not reached the collapse resistance limit state under the action of rare earthquakes. The larger the R , the stronger the collapse resistance of the structure. The larger the safety reserve, the safer the structure. When $R = 1$, it indicates that the structure has just reached the collapse resistance limit state under the action of a rare earthquake, the structure has no safety reserve, and the structure may collapse if the earthquake action increases. When $R < 1$, it indicates that the structure has exceeded the collapse resistance limit state under the action of a rare earthquake, and the structure has collapsed, which is an unsafe structure.

2.3. Material Constitutive Model Based on Structural Elastoplastic Analysis. In the nonlinear analysis of reinforced concrete structures, the constitutive relationship model of concrete has a significant influence on the analysis results. In the actual reinforced concrete structure engineering, the coupling beam and the floor are connected by the reinforcement, and the coupling beam and the floor are poured at one time. Therefore, the contribution of the floor to the stiffness of the coupling beam must be considered in the calculation of the concrete structure; that is, the coupling beam is regarded as a T-beam. The floor is made of isotropic materials, and the elastic modulus is the elastic modulus of concrete. The floor unit has no bending stiffness and can only output the stress and strain in two directions in the unit plane. Multilayer composite materials are not supported. The concrete layer in the shear wall is generally two-dimensional, and the edge-constrained components are even three-dimensional. The constitutive model is much more complicated than the fiber model. For general engineering applications, the classic concrete elastoplastic + fracture constitutive model has a small amount of calculation and its accuracy can meet engineering needs. This paper mainly adopts the concrete constitutive model defined in MSC.MARC. The elastoplastic behavior of concrete materials in this model is based on the classical incremental elastoplastic constitutive theory, while the fracture behavior of concrete is described by a diffuse crack model.

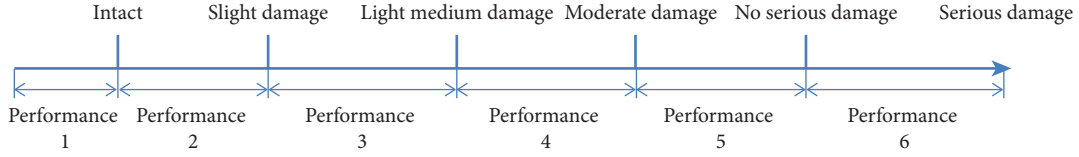


FIGURE 1: Performance division diagram of members under bending or bending shear failure.

The numerical model adopted for reinforcement is expressed as

$$f = \beta\sqrt{3}\bar{\sigma}I_1 + \gamma I_1^2 + 3J_2 - \bar{\sigma}^2 = 0. \quad (5)$$

In the equation, $I_1 J_2$ is the first invariant of stress tensor and the second invariant of stress deflection. According to the expression of the numerical model, the parameter value is $\beta = 3, \gamma = 0.2$.

In this model, the incremental elastoplastic constitutive relationship is adopted, and the flow law is the associated flow. According to the $\sigma - \varepsilon_p$ (stress-plastic strain) curve of concrete under uniaxial compression, and according to the conversion relationship of (6) and (7), we obtain the equivalent stress-equivalent plastic strain relationship curve to calculate the hardening law.

$$\bar{\sigma} = \frac{\sigma}{2.8}, \quad (6)$$

$$\bar{\varepsilon}_p = \sqrt{3}\varepsilon_p. \quad (7)$$

In the equation, $\bar{\sigma}$ and $\bar{\varepsilon}_p$ are the equivalent stress and equivalent plastic strain, respectively.

According to the incremental elastoplastic constitutive theory, the calculated hardening equation after yield is

$$d\sigma = \left[D_e - \frac{D_e \{ \partial f / \partial \sigma \} \{ \partial f / \partial \sigma \} D_e}{(1 - 3J_1/2\bar{\sigma})H' + \{ \partial f / \partial \sigma \} D_e \{ \partial f / \partial \sigma \}} \right] d\varepsilon \quad (8)$$

$$= D_p d\varepsilon.$$

In the equation, D_e is the elastic constitutive matrix of the material, and the parameter H' is the hardening parameter.

The main parameters that need to be set in the material constitutive model are shown in Figure 2. Since this model is based on the classic elastoplastic mechanics theory, the yield stress σ_y of the material needs to be set. The uniaxial compression test of concrete shows that for general concrete, before the stress reaches $(0.3 \sim 0.4)f_c$, the deformation of the specimen is mainly elastic deformation, and the compressive stress-strain relationship is approximately straight. Therefore, the yield stress σ_y of concrete materials can generally be set to the peak strength 1/3 of it.

It can be seen from Figure 2 that the constitutive model is a mathematical model defining the mechanical properties of a material. In short, it is the response of the material receiving external excitation, and it is also the stress-strain relationship. Different materials have different constitutive models, which can be compiled into different types of material subroutines, which exist independently of other modules of finite element analysis.

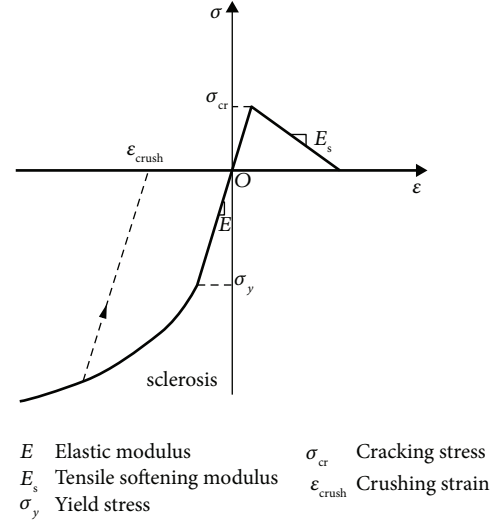


FIGURE 2: Schematic diagram of constitutive model parameters.

2.4. Model Optimization Based on Response Surface Methodology. This paper proposes a new optimization method for complex constitutive models, a model optimization method based on the response surface method, and uses the response surface method to optimize the material constitutive model constructed above. In this optimization, the axial compression ratio of the shear wall and the shear claw ratio of the beam are used as constraints to control the component indexes, and the structural displacement ratio, displacement angle, and period ratio are used as constraint conditions to control the overall index. Regarding both the positive analysis results and the measured results as prior knowledge, the design parameter values are changed through experimental design, the numerical calculation model is used for positive analysis to obtain typical sample points, and an equivalent fast-running model-response surface is established through statistical learning methods. The model is used to replace the original numerical calculation model for structural analysis to reduce the computational complexity in the model optimization process and to find the global optimal solution of the structural design parameters. The principle of constitutive model optimization based on response surface is to select some appropriate structural parameter values within a reasonable range of structural parameters, use the structural numerical calculation model to calculate the response value, and fit the structural response value and structural parameters with an explicit response surface function; a simplified structural response surface model is obtained based on the complex implicit relationship between the structure response surface model [30].

The parametric model optimization method can be expressed as follows: optimizing the structural parameters x_1, x_2, \dots, x_n (geometric size, elastic modulus, elastic stiffness, damping coefficient, etc.) to use the finite element model to calculate the structural performance index y (displacement, displacement angle, period, etc.) consistent with actual test results. For this reason, it is necessary to study the quantitative relationship between y and x_1, x_2, \dots, x_n , and the relationship between them can be expressed by the model shown in

$$y = f(x_1, x_2, \dots, x_n) + \varepsilon. \quad (9)$$

In the equation, $f(x_1, x_2, \dots, x_n)$ is a function of x_1, x_2, \dots, x_n , usually called the response function, and ε is a random error, which represents the interference term caused by the influence of uncontrollable noise factors. It is usually assumed that ε is independent of each other in different experiments. And the mean is 0, and the variance is σ^2 . Because the relationship between response y and x_1, x_2, \dots, x_n can be graphically described as a curved surface on the area of x_1, x_2, \dots, x_n , the study of this relationship is called response surface.

Usually, the purpose of research is to maximize or minimize the response or achieve the desired response value. This article is divided into two stages.

The main goal of the first stage is to determine whether the current test conditions or the level of input variables are close to the optimal (maximum or minimum) position of the response surface. When the test conditions are far away from the optimal position of the surface, the first-order model is usually used to approximate:

$$y = \alpha_0 + \sum_{i=1}^n \alpha_i x_i + \varepsilon. \quad (10)$$

In the equation, the undetermined coefficient α_i represents the slope or linear effect of variable x_i .

When the test area is close to the optimal area of the response surface or is located in the optimal area, the second stage design can be carried out; the purpose is to obtain an accurate approximation of the response surface near the optimal value and identify the optimal level combination of input variables. At this time, the second-order model is often used to approximate:

$$y = \alpha_0 + \sum_{i=1}^n \alpha_i x_i + \sum_{i=1}^n \sum_{j=1}^n \alpha_{ij} x_i x_j + \varepsilon. \quad (11)$$

The optimized constitutive model parameters are obtained by iterative optimization according to the measured response value of the structure test. The optimization calculation directly based on the explicit polynomial response surface function is completely a mathematical operation process, which can significantly improve the optimization efficiency and reduce the number of numerical analysis calculations. Therefore, the response surface model is a fast-running model.



FIGURE 3: Architectural rendering.

3. Simulation Experiment Analysis

In order to verify the performance of the dual-line-of-defense seismic performance analysis method of super high-rise buildings based on the response surface optimization algorithm in practical applications, a simulation experiment was carried out. This paper takes an actual super high-rise building project located in the center of Zhengzhou, Henan Province, as the research background. This project is a 45-story super high-rise commercial building, which is used for commercial and office use. The main building has 4 underground floors and is integrally connected to the 4-story underground garage. The main building and the commercial podium are equipped with expansion joints and seismic joints. The appearance of the building is shown in Figure 3. The total height of the main building is 176.3 m, the plane size is 34.4 m \times 54.0 m, the core barrel size is 13.6 m \times 22.0 m \times 8 m, the main building adopts the form of grouting bored pile + raft foundation, and the software used is design expert V8.0.6. The seismic fortification intensity of the project site is 7°, the design seismic acceleration value is 0.15 g, the design earthquake group is the second group, the design characteristic period is 0.40 s, and the category of the construction site is class II.

Among them, the actual reinforcement diagram of the shear wall and beam members is shown in Figure 4.

According to the above super high-rise building structure, shear wall, and reinforcement structure of beam members, the structural calculation parameters are obtained, as shown in Table 1.

The optimization model in this paper is used to optimize the shear wall and beam components, and the maximum axial compression ratio of the shear wall and beam components is compared with the specification limit. The comparison result is shown in Figure 5.

According to Figure 5, during the optimization process, the axial compression ratio of the wall column is always relatively stable. The column is always around 0.5 and the wall is around 0.26.



FIGURE 4: Actual reinforcement diagram of shear wall and beam members. (a) Actual reinforcement drawing of the shear wall. (b) Actual reinforcement drawing of the beam member.

TABLE 1: Structural calculation parameters.

Name	Parameter
Maximum control length of wall panel subdivision (m)	0.8
Minimum control length of wall panel subdivision (m)	0.8
Earthquake intensity	7.5 (0.15 g)
Site type	II
Design earthquake grouping	The second group
Characteristic period	0.45
Explicit analysis of vertical loading	Yes
Mode number of modal calculation	10

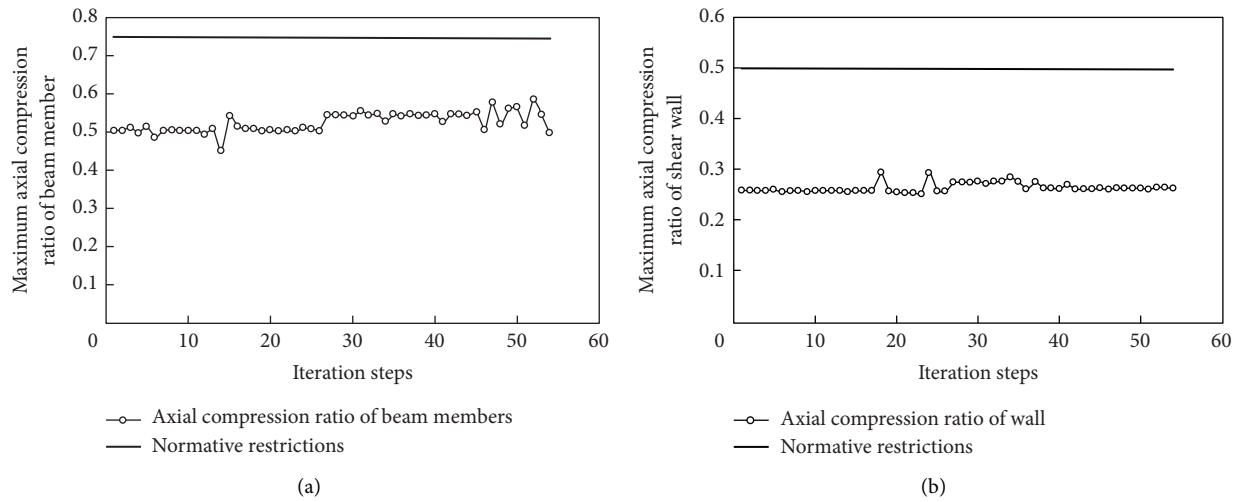


FIGURE 5: Comparison results of the maximum axial compression ratio of beam members and shear walls. (a) Axial compression ratio of the beam member. (b) Axial compression ratio of shear wall.

The optimization model in this paper is used to optimize the total weight of the super high-rise building structure, and the total weight of the structure is compared with the specification limit. The comparison result is shown in Figure 6.

In the first 26th step of the optimization process, the total weight curve of the structure developed smoothly, fluctuating between 372207 kN and 379033 kN, rapidly decreased

to 342530 kN at the 27th step, and reached the minimum value of 328699 kN at the 34th step, but at this time, the beam shear-compression ratio exceeded. According to the specification limit, the shear force distribution ratio of the first-story frame is less than 10% of the constraint requirement, and then, the weight curve rises slightly to 353862 kN and then develops relatively smoothly, reaching convergence in step 54.

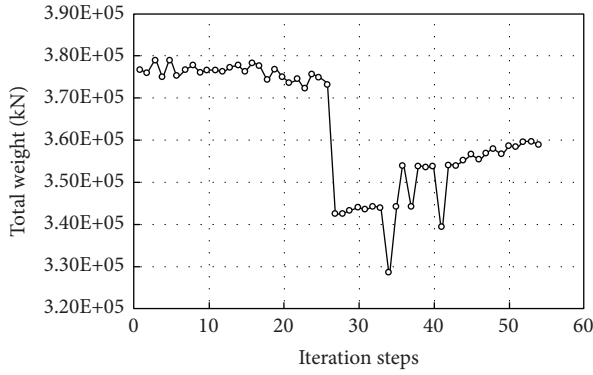


FIGURE 6: Comparison of total structural weight.

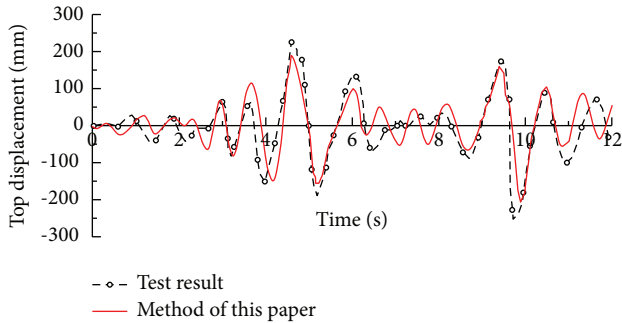


FIGURE 7: Time history curve of structural vertex displacement.

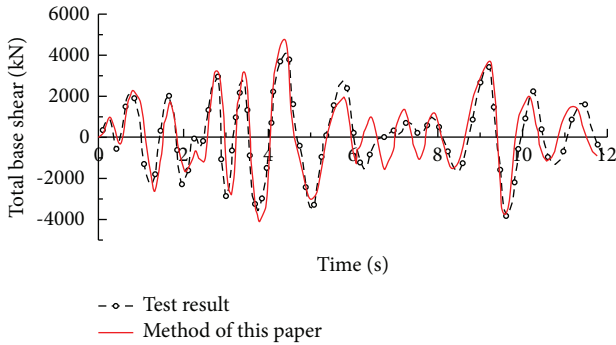


FIGURE 8: Time history curve of structural base shear force.

The method in this paper is used to obtain the time history results of the top floor displacement and the total base shear force and compare them with the actual test results. The time history curve of the top displacement of the super high-rise building structure and the time history curve of the total base shear force are drawn through Matlab simulation software, as shown in Figures 7 and 8.

The seismic response of the super high-rise building structure is simulated and analyzed accurately. From the time history calculation results of the top floor displacement and the total base shear force, it can be basically consistent with the actual test results, especially the peak response time.

4. Conclusion

With the rapid development of the world economy, people's needs and pursuits for life continue to increase, along with the deepening of economic globalization, coupled with factors such as urban population concentration, land shortage, and fierce business competition, a large number of high-level, super high-rise buildings are widely used at home and abroad, and they are mainly used in commercial, residential, hotel, and other fields. The research and development of building materials, the research of new structural systems, and the rapid development of computer operation speed have provided the possibility for the design and construction of high-rise buildings. The continuous development of new building materials, new structural forms, and building construction technologies, as well as the continuous updating and development of computer technology, provide solid technical support for the design and construction of super high-rise buildings. The following conclusions were drawn from the research:

- (1) Research on the seismic performance of double defense lines of super high-rise building structures based on the response surface optimization algorithm. During the optimization process, the axial compression ratio of the wall and column changes steadily, the column is always around 0.5, and the wall is always around 0.26
- (2) The overall weight curve of the structure develops smoothly during the optimization process
- (3) The time history calculation results of the top floor displacement and the total shear force of the base of the super high-rise building structure basically agree with the actual test results, especially the time when the peak response occurs.

However, due to the frequent occurrence of earthquake disasters and the continuous rise of building heights, while the structural design and construction of super high-rise buildings are becoming more difficult, the analysis of the seismic performance of super high-rise building structural systems and the research on high-efficiency seismic structural systems have become particularly critical. Improving the overall seismic performance of supertall building structures in China has far-reaching implications for the construction industry. Future research can further analyze the following aspects:

- (1) The next step is to compare and analyze the results of the calculation examples with different intensities and heights. In the future, further calculation and comparison of more calculation examples are needed to demonstrate the rationality of the results.
- (2) Due to the lack of data statistics (number of non-structural components, quota, construction period, etc.), the next work can evaluate the postearthquake repair cost, repair time, and casualties of the structure. Subsequent research can also count the cost of components and the number of nonstructural

components corresponding to different building functions, so as to further improve the research on seismic toughness evaluation.

Data Availability

The datasets used and/or analyzed during the current study can be obtained from the corresponding author upon reasonable request.

Conflicts of Interest

The authors declare that there are no conflicts of interest.

References

- [1] M. Buitrago, P. A. Calderón, J. J. Moragues, Y. A. Alvarado, and J. M. Adam, "Load limiters on temporary shoring structures: tests on a full-scale building structure under construction," *Journal of Structural Engineering*, vol. 147, no. 3, pp. 40–45, 2021.
- [2] M. Hill, E. Nijkamp, and S. C. Zhu, "Building a telescope to look into high-dimensional image spaces," *Quarterly of Applied Mathematics*, vol. 77, no. 2, pp. 269–321, 2019.
- [3] C. Tang, Y. M. Li, and B. W. Xu, "Evaluation of seismic performance of RC frame-shear wall structure with different stiffness eigenvalues based on multi-criteria," *Structural Engineer*, vol. 35, no. 2, pp. 149–157, 2019.
- [4] Z. Alam, L. Sun, C. W. Zhang, Z. X. Su, and B. Samali, "Experimental and numerical investigation on the complex behaviour of the localised seismic response in a multi-storey plan-asymmetric structure," *Structure and Infrastructure Engineering*, vol. 17, no. 1, pp. 86–102, 2020a.
- [5] W. Zhang, X. Liu, Y. Huang, and M. N. Tong, "Reliability-based analysis of the flexural strength of concrete beams reinforced with hybrid BFRP and steel rebars," *Archives of Civil and Mechanical Engineering*, vol. 22, no. 4, p. 171, 2022.
- [6] H. Huang, M. Guo, W. Zhang, and M. Huang, "Seismic behavior of strengthened RC columns under combined loadings," *Journal of Bridge Engineering*, vol. 27, no. 6, 2022.
- [7] J. Li, Q. Fan, Z. Lu, and Y. Wang, "Experimental study on seismic performance of T-shaped partly precast reinforced concrete shear wall with grouting sleeves," *The Structural Design of Tall and Special Buildings*, vol. 28, no. 13, pp. e1632.1–e1632.13, 2019.
- [8] X. Ma, J. Ma, and Y. Yue, "Experimental and numerical investigation on seismic performance of a hybrid RC frame system with stiffened masonry wall," *Journal of Advanced Concrete Technology*, vol. 16, no. 12, pp. 600–614, 2018.
- [9] Z. Alam, C. Zhang, and B. Samali, "The role of viscoelastic damping on retrofitting seismic performance of asymmetric reinforced concrete structures," *Earthquake Engineering and Engineering Vibration*, vol. 19, no. 1, pp. 223–237, 2020b.
- [10] J. Li, "Seismic performance analysis of over-limit high-rise structures under moderate earthquakes — a special case evaluation of Changsha Fusheng Financial Center," *Fujian Architecture*, vol. 36, no. 11, pp. 15–20, 2019.
- [11] W. J. Yi and W. W. Zhou, "Seismic performance analysis of frame-shear wall structure with different frame overturning moment ratio," *Building Structure*, vol. 36, no. 9, pp. 48–54, 2019.
- [12] T. F. Voica and A. Stratan, "Review of damage-tolerant solutions for improved seismic performance of buildings," *IOP Conference Series: Materials Science and Engineering*, vol. 789, no. 1, Article ID 012062, 2020.
- [13] R. Suwondo, D. Mangindaan, L. Cunningham, and S. Alama, "Non-linear analysis of seismic performance of low-rise concrete buildings in Indonesia," *IOP Conference Series: Earth and Environmental Science*, vol. 794, no. 1, Article ID 012024, 2021.
- [14] Z. Alam, L. Sun, C. Zhang, and B. Samali, "Influence of seismic orientation on the statistical distribution of nonlinear seismic response of the stiffness-eccentric structure," *Structures*, vol. 39, pp. 387–404, 2022.
- [15] A. Donyaii, "Evaluation of climate change impacts on the optimal operation of multipurpose reservoir systems using cuckoo search algorithm," *Environmental Earth Sciences*, vol. 80, no. 19, p. 663, 2021.
- [16] S. Huang and C. Liu, "A computational framework for fluid-structure interaction with applications on stability evaluation of breakwater under combined tsunami-earthquake activity," *Computer-Aided Civil and Infrastructure Engineering*, 2022, n/a(n/a).
- [17] J. B. Li, F. Cheng, G. Lin, and C. L. Wu, "Improved hybrid method for the generation of ground motions compatible with the multi-damping design spectra," *Journal of Earthquake Engineering*, pp. 1–27, 2022.
- [18] S. Huang, M. Huang, and Y. Lyu, "Seismic performance analysis of a wind turbine with a monopile foundation affected by sea ice based on a simple numerical method," *Engineering Applications of Computational Fluid Mechanics*, vol. 15, no. 1, pp. 1113–1133, 2021a.
- [19] Z. Lin, H. Wang, and S. Li, "Pavement anomaly detection based on transformer and self-supervised learning," *Automation in Construction*, vol. 143, Article ID 104544, 2022.
- [20] Y. T. Bai, S. H. Wang, B. Mou, Y. Wang, and K. A. Skalomenos, "Bi-directional seismic behavior of steel beam-column connections with outer annular stiffener," *Engineering Structures*, vol. 227, Article ID 111443, 2021.
- [21] S. Huang, Y. Lyu, H. Sha, and L. Xiu, "Seismic performance assessment of unsaturated soil slope in different groundwater levels," *Landslides*, vol. 18, no. 8, pp. 2813–2833, 2021b.
- [22] Z. Cao and Q. Li, "Effect of connection deficiency on seismic performance of precast concrete shear wall-frame structures," *Journal of Earthquake and Tsunami*, vol. 13, no. 03n04, pp. 1940005–1941261, 2019.
- [23] N. Lu, H. Wang, K. Wang, and Y. Liu, "Maximum probabilistic and dynamic traffic load effects on Short-to-Medium Span Bridges," *Computer Modeling in Engineering and Sciences*, vol. 127, no. 1, pp. 345–360, 2021.
- [24] J. Li, Y. Wang, Z. Lu, and B. Xia, "Shaking table test and numerical simulation of a superimposed reinforced concrete shear wall structure," *The Structural Design of Tall and Special Buildings*, vol. 27, no. 2, pp. e1412–e1416, 2018.
- [25] L. M. Jiang, J. Zhu, C. Liu, and L. J. Xiao, "Study on seismic performance of RC shear wall structure strengthened with HPFL under different axial compression ratio," *Journal of Hefei University of Technology*, vol. 41, no. 6, pp. 822–827, 2018.
- [26] P. PanPan, S. J. Wu, H. S. Wang, and X. NieNie, "Seismic performance evaluation of an infilled rocking wall frame structure through quasi-static cyclic testing," *Earthquake Engineering and Engineering Vibration*, vol. 17, no. 2, pp. 371–383, 2018.
- [27] Z. Zhang and Y. Zhang, "Research status on reinforcement connection form of precast concrete shear wall structure,"

- IOP Conference Series: Materials Science and Engineering*, vol. 322, no. 4, Article ID 042001, 2018.
- [28] Z. Chen, X. Zhou, X. Wang, P. Zhao, and J. Hu, "Dynamic behavior of super high-rise building: deployment of smart monitoring system and analysis," *Journal of Structural Engineering*, vol. 146, no. 4, pp. 1–12, 2020.
- [29] Y. Du, J. Hao, J. Yu et al., "Seismic performance of a repaired thin steel plate shear wall structure," *Journal of Constructional Steel Research*, vol. 151, no. 12, pp. 194–203, 2018.
- [30] Y. Luo, H. Zheng, H. Zhang, and Y. Liu, "Fatigue reliability evaluation of aging prestressed concrete bridge accounting for stochastic traffic loading and resistance degradation," *Advances in Structural Engineering*, vol. 24, no. 13, pp. 3021–3029, 2021.